NONLINEAR OSCILLATORY CONVECTION: A QUANTITATIVE PHASE DYNAMICS APPROACH

S. FAUVE, E.W. BOLTON* and M.E. BRACHET**
Groupe de Physique des Solides de l'Ecole Normale Supérieure, 24, rue Lhomond 75231, Paris Cedex 05, France

The oscillatory instability of convective rolls, for both free-slip and rigid boundary conditions, is shown to be related to the translational and Galilean invariances of the Oberbeck–Boussinesq equations, which implies that the phase dynamics of the basic roll pattern is *second order* in time. In the free-slip case the invariance is exact and the instability comes in at zero wavenumber. It is argued that, for low Prandtl number fluids, the effect of the rigid boundaries is to *weakly* break the Galilean invariance, thereby shifting the instability's critical wavenumber to a finite value. We derive the equations governing the nonlinear phase dynamics and show that, when supercritical, the instability always saturates into *travelling waves* (as observed in experiments and numerical simulations). In the rigid case, the description is made quantitative by numerically computing both the linear and nonlinear coefficients of the phase equation. It is found that, depending of the values of Prandtl number P and basic roll pattern wavenumber α, the oscillatory instability can be supercritical or subcritical. In the case of mercury ($P = 0.025$), our model predicts transition from supercritical onset to subcritical onset, for α slightly below the critical wavenumber for convection onset.

1. Introduction

In many nonlinear dissipative systems driven far from equilibrium by an external homogeneous forcing, there is a transition from a uniform state to one varying periodically in space. A widely studied example is the Rayleigh–Bénard instability that occurs in a fluid layer heated from below; when the temperature difference across the layer exceeds a critical value, the buoyancy force overcomes the dissipative effects of viscous shear and thermal conduction, and the motionless state spontaneously breaks up into convective cells. With Boussinesq fluids, and when the temperature is fixed at the top and bottom boundaries, a parallel roll pattern is selected at the convection onset in a laterally infinite fluid layer [1]. The stability of these rolls as a function of their wave-

number, the Rayleigh number and the Prandtl number, has been carefully studied by Galerkin techniques [2–5].

Another possible approach is to investigate the stability and the dynamics of periodic patterns through their slowly varying phase [6]. A spatially uniform modification of the phase corresponds to a shift of the roll pattern, and thus is neutral because of translational invariance. Correspondingly, the growth-rate for the phase modes describing long wavelength perturbations of the roll pattern is small. Therefore the basic idea is to eliminate adiabatically the fast modes and to obtain an evolution equation for the phase. This method has been used to describe pattern dynamics in time periodic chemical reactions [7–9], and to study the stability of cellular flows which arise in Rayleigh–Bénard convection or Couette–Taylor flow. Most of the long wavelength instabilities of convective rolls, found with a Galerkin technique [2, 3], have been recovered, at least qualitatively, with the concept of phase dynamics

*Present address: Department of Geology and Geophysics, Yale University, Box 6666, New Haven, CT 06511, USA.
**Also, Observatoire de Nice, B.P. 139, 06003 Nice, France.

[10–12], except for the oscillatory instability, which is the most dangerous one for low Prandtl number fluids (liquid metals, for instance). The oscillatory instability consists of a transverse oscillation of the rolls which propagates along their axis. It is connected with the appearance of vertical vorticity [13, 14]. Its critical wavenumber vanishes in the case of stress-free top and bottom boundary conditions [13], and is finite for rigid boundary conditions [2, 15]. It was pointed out recently that a possible mechanism for propagative phase dynamics is a mean flow effect due to Galilean invariance [16]. We show in this paper that there is a similar effect for the oscillatory instability, and that the method of phase dynamics gives quantitative results on the nonlinear oscillatory regime.

This paper is organized in the following fashion. In section 2 we consider convective rolls with stress-free boundary conditions and give the phase equations which describe the dynamics of long wavelength torsion modes of the pattern. In section 3 we extend our analysis to the more experimentally accessible case of rigid boundary conditions; in that case the Galilean invariance is externally broken by the boundaries; however this only slightly modifies our analysis in the small Prandtl number limit. We give the nonlinear evolution equation describing the oscillatory instability, and show that, if supercritical, it takes the form of propagative waves, as observed experimentally [17] and in direct numerical simulations [18–20, 27]. In section 4, we compare our model with a stability analysis using a Galerkin technique, and compute numerically the coefficients of the phase equation. We show that the oscillatory instability can be supercritical or subcritical, depending on the Prandtl number and the basic pattern wavenumber.

2. Phase equations for stress-free boundary conditions

We consider a horizontal fluid layer of depth d, of infinite extension in the horizontal plane, heated from below; the fluid's kinematic viscosity is ν and its thermal diffusivity is κ. Using d, d^2/κ and the temperature difference ΔT across the layer, divided by the Rayleigh number R, as scales for length, time and temperature, the conservation equations for mass, momentum and heat, read in the Oberbeck–Boussinesq approximation,

$$\nabla \cdot v = 0, \tag{1a}$$

$$\partial_t v + v \cdot \nabla v = -P\nabla p + P\nabla^2 v + P\Theta z, \tag{1b}$$

$$\partial_t \Theta + v \cdot \nabla \Theta = Rv \cdot z + \nabla^2 \Theta. \tag{1c}$$

where $v = (u, v, w)$ is the velocity vector, Θ is the temperature deviation from the linear profile, and p represents the pressure disturbances; z is the vertical unit vector opposite to gravity. Two dimensionless numbers characterize the problem: the Rayleigh number R, and the Prandtl number P,

$$R = g\gamma d^3 \Delta T/\nu\kappa, \quad P = \nu/\kappa,$$

where g is the acceleration of gravity and γ is the isobaric thermal expansion coefficient.

Two different kinds of boundary conditions are usually considered for the above set of equations. In the case of stress-free boundary conditions, one requires

$$w = \partial_z u = \partial_z v = 0 \quad \text{at} \quad z = 0, 1, \tag{2a}$$

whereas for rigid boundaries one has

$$v = 0 \quad \text{at} \quad z = 0, 1. \tag{2b}$$

If the heat conductivity of the boundaries is large compared to the one of the fluid, one has

$$\Theta = 0 \quad \text{at} \quad z = 0, 1. \tag{2c}$$

At the convective onset, the only possible stable steady solution of eqs. (1) with the boundary conditions (2) consists of two-dimensional rolls [1], taken without loss of generality to have the

form

$$U_0(x, z)$$
$$= [u_0(x, z), 0, w_0(x, z), p_0(x, z), \theta_0(x, z)].$$
$$(3)$$

Translational symmetry in the horizontal plane implies that $U_0(x + \phi, z)$ is also a solution, and consequently $\partial_x U_0$ is a neutral mode of the roll pattern described by (3).

With stress-free boundary conditions another neutral mode exists, which consists of a uniform horizontal velocity ψ along the x-axis. In order to investigate the linear structure of this instability, let us consider a perturbation of the basic pattern of the form

$$U(x, z, t) = U_0[x + \phi(t), z] - \psi(t)I, \qquad (4)$$

where $I = (1, 0, 0, 0, 0)$. We obtain from (1) and (4)

$$\phi_t \, \partial_x U_0 - \psi_t I = \psi \, \partial_x U_0$$

or

$$\partial_t \begin{pmatrix} \phi \\ \psi \end{pmatrix} = \begin{pmatrix} 0 & 1 \\ 0 & 0 \end{pmatrix} \begin{pmatrix} \phi \\ \psi \end{pmatrix}. \qquad (5)$$

The linear phase dynamics is thus second order in time. The existence of two phase modes ϕ and ψ is related to translational and Galilean invariances; their linear coupling can be understood as follows: the advection of the pattern at a constant speed ψ along the x-axis leads to a spatial phase ϕ that increases linearly in time. This makes the phase dynamics second order in time, which can give rise to propagative behavior for long wavelength disturbances of the periodic pattern. It is indeed known that for low Prandtl number fluids ($P \ll 1$), a propagative torsion mode of the roll pattern is amplified close to the convection onset, and gives rise to the oscillatory instability [13]; the roll pattern is shifted perpendicular to its axis, periodically along the axis and in time (see fig. 1)
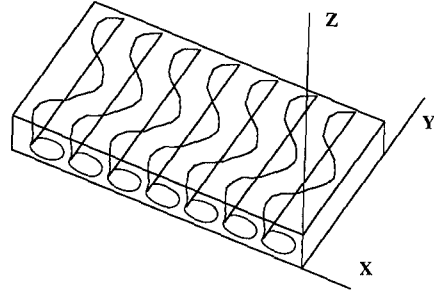

Fig. 1. Qualitative sketch of the oscillatory instability of convective rolls.

In order to explain this behavior, let us consider a perturbation of the basic pattern in the form

$$U(x, y, z, t) = U_0[x + \phi(Y, T), z] - \psi(Y, T)I$$
$$+ u(x, z, Y, T), \qquad (6)$$

where $\phi(Y, T)$ represents a long wavelength modulation of the spatial phase along the roll axis, and $\psi(Y, T)$ is a slowly varying horizontal velocity; the corresponding vertical vorticity mode was first considered by Busse in his stability analysis of two-dimensional convective rolls in a low Prandtl number fluid [13]. It was shown by Siggia and Zippelius [14] that this mode also modifies at leading order the evolution equation which governs the roll amplitude in the vicinity of the convection onset [21, 22].

In the limit of zero wavenumber, eq. (6) reduces to (4), and the evolution of $\phi(T)$ and $\psi(T)$ is governed by eq. (5), which represents a codimension-two singularity [23, 24]; the structure of the Galilee group implies that the eigenmode $\partial_x U_0$ has a double zero eigenvalue. The first part of expression (6) consists of a perturbation of the basic state $U_0(x, z)$ along the generalized eigenspace $\{\partial_x U_0, I\}$, whereas $u(x, z, Y, T)$ stands for corrections perpendicular to this eigenspace. In the long wavelength limit, the eigenmodes are almost neutral; therefore we assume that all other modes behave on time scales much faster than the ones of ϕ and ψ, and thus can be eliminated to give evolution equations for ϕ and ψ, which can be set

under the form

$$\phi_T = \psi + f(\phi, \psi, \partial_Y), \tag{7a}$$

$$\psi_T = g(\phi, \psi, \partial_Y). \tag{7b}$$

At this point let us remark that, as shown by Siggia and Zippelius [14], and Cross [11], the dependence of the amplitude equations on the slowly varying horizontal velocity ψ is singular when ψ depends on X and Y. In order to avoid this problem, we must consider only Y-dependent ϕ and ψ with decoupled dynamics at zero wavenumber.

– The first condition amounts to consider only the oscillatory instability: our model thus ignores the skew-varicose and oscillatory skew-varicose instabilities which involve X- and Y-dependent perturbations. Its validity is thus restricted to situations where the first instability of the convection rolls is the oscillatory instability.

– The second condition reads

$$\bar{\phi}_T = 1/(2L) \, \partial_T \int_{-L}^{L} \phi(Y, T) \, dY = \bar{\psi}, \tag{8a}$$

$$\bar{\psi}_T = 1/(2L) \, \partial_T \int_{-L}^{L} \psi(Y, T) \, dY = 0. \tag{8b}$$

It amounts to decouple Y-dependent perturbations from the singular X-dependent modes in the zero wavenumber limit ($k_x = k_y = 0$). Let us remark that (8b) traces back to the conservation of the horizontal momentum, which forbids a change in the global advection of patterns along the x-axis.

Let us next assume that f, g and u can be expanded in multiple Taylor series of ϕ, ψ, and their gradients. The compatibility between (1), (6) and (7) gives evolution equations for ϕ and ψ at each order in the gradient expansion. Their form is determined by symmetry constraints:

– Translational and Galilean invariances imply the invariance of the equations under the transformations

$\phi \rightarrow \phi + c$ (where c is constant),

$\phi \rightarrow \phi + ct,$ $\psi \rightarrow \psi + c,$

thus f and g depend on ϕ and ψ only through their Y-derivatives.

– Space reflection symmetry implies the invariance of the phase equations under the transformations

$$x \rightarrow -x, \quad \phi \rightarrow -\phi, \quad \psi \rightarrow -\psi$$

and

$$Y \rightarrow -Y.$$

It follows from the first constraint that f and g involve no quadratic nonlinearities. The second one implies that the number of Y-derivatives is even for each term of f and g. These symmetry constraints, together with conditions (8) for periodic boundary conditions along the Y-axis, imply that eqs. (7), up to third order in ϕ and ψ and fourth order in ∂_Y, are of the form

$$\phi_T = \psi + \partial_Y \left[\alpha \phi_Y + \beta \psi_Y + \gamma \phi_{YYY} + \delta \psi_{YYY} \right. $$
$$\left. + \gamma_1 \phi_Y^3 + \gamma_2 \phi_Y^2 \psi_Y + \gamma_3 \phi_Y \psi_Y^2 + \gamma_4 \psi_Y^3 \right], \tag{9a}$$

$$\psi_T = \partial_Y \left[\alpha' \phi_Y + \beta' \psi_Y + \gamma' \phi_{YYY} + \delta' \psi_{YYY} \right. $$
$$\left. + \gamma_1' \phi_Y^3 + \gamma_2' \phi_Y^2 \psi_Y + \gamma_3' \phi_Y \psi_Y^2 + \gamma_4' \psi_Y^3 \right]. \tag{9b}$$

We next observe that the differentiated terms of (9a) and the last terms of (9b) are non-resonant and can be eliminated at this order by the following change of variables:

$$\phi = \tilde{\phi} + \left[(\gamma_2 + \gamma_3'/2)/3 \right] \left(\tilde{\phi}_Y^3 \right)_Y$$
$$+ \left[(\gamma_3 + \gamma_4')/2 \right] \left(\tilde{\phi}_Y^2 \tilde{\psi}_Y \right)_Y,$$

$$\psi = \tilde{\psi} - \alpha \tilde{\phi}_{YY} - \beta \tilde{\psi}_{YY} + (\alpha\beta - \gamma) \tilde{\phi}_{YYYY}$$
$$+ (\beta^2 - \delta) \tilde{\psi}_{YYYY} - \gamma_1 \left(\tilde{\phi}_Y^3 \right)_Y$$
$$+ (\gamma_3'/2) \left(\tilde{\phi}_Y^2 \tilde{\psi}_Y \right)_Y + \gamma_4' \left(\tilde{\phi}_Y \tilde{\psi}_Y^2 \right)_Y - \gamma_4 \left(\tilde{\psi}_Y^3 \right)_Y$$

Finally we write $\theta = \tilde{\phi}_Y$, and $\chi = \tilde{\psi}_Y$, the phase

gradients, and obtain

$$\theta_T = \chi, \tag{10a}$$

$$\chi_T = \partial_{YY}\big[a\theta + b\chi - c\theta_{YY} - d\chi_{YY} + g_1\theta^3 + g_2\theta^2\chi\big], \tag{10b}$$

where

$a = \alpha',$
$b = \alpha + \beta',$
$c = \alpha\beta' - \alpha'\beta - \gamma',$
$d = -\gamma - \delta',$
$g_1 = \gamma_1',$
$g_2 = 3\gamma_1 + \gamma_2'.$

Eqs. (10) describe the stability of the roll pattern with respect to long wavelength perturbations, i.e. θ and χ varying like $\exp(\eta T \pm ikY)$ with $k \to 0$. In this limit the dispersion relation is

$$\eta^2 + bk^2\eta + ak^2 = \mathcal{O}(k^2), \tag{11}$$

where the coefficients depend on the Rayleigh number R, the Prandtl number P, and the wavenumber α of the basic roll pattern. The oscillatory instability occurs when $b(R, P, \alpha)$ vanishes i.e. on the critical surface $R = R_0(P, \alpha)$ of the R–P–α space. Its frequency at onset is

$$\omega_0 = k\sqrt{a}(R_0, P, \alpha).$$

In the vicinity of the instability onset, we have

$$\eta = \pm ik\sqrt{a} - bk^2/2 + \cdots.$$

The coefficients a and b have been computed by Busse (see ref. [13], eq. (3.11) for $\sigma_1 = i\sqrt{a}$, and eq. (3.17) for $\sigma_2 = -b/2$).

The nonlinear terms of eq. (10b) simply renormalize the damping and the frequency of the instability, which is a supercritical Hopf bifurcation if $g_2 > 0$. We can compute the coefficients of the nonlinear terms by noting that $\theta = p$ is a particular solution of (10), which corresponds to a

slight rotation of the roll pattern. We consider

$$\theta = p + \varepsilon\exp(\eta T + ikY)$$

and linearize eqs. (10) in ε. We obtain

$$\eta^2 + \big[b(\alpha) + g_2 p^2\big]k^2\eta + \big[a(\alpha) + 3g_1 p^2\big]k^2 = \mathcal{O}(k^2). \tag{12}$$

The wavenumber of the slightly rotated pattern described by $\theta = p$, is

$$\alpha' \approx \alpha(1 + p^2/2). \tag{13}$$

We can also write the dispersion relation which gives the growth-rate of the slightly rotated pattern, in the form

$$\eta^2 + b(\alpha + \alpha p^2/2)k^2\eta + a(\alpha + \alpha p^2/2)k^2 = \mathcal{O}(k^2). \tag{14}$$

We obtain from (12) and (13)

$$g_1 = (\alpha/6)\,\partial a/\partial\alpha, \tag{15a}$$

$$g_2 = (\alpha/2)\,\partial b/\partial\alpha. \tag{15b}$$

Thus the nonlinear effects can be understood as follows: the wavy disturbances slightly modify the local wavenumber (see eq. (13)), and in turn, this changes locally the propagation speed and the damping rate of the disturbances.

3. Phenomenological extension to rigid boundary conditions

3.1. The oscillatory instability growth-rate

In most experimental realizations of thermal convection, the top and bottom boundaries are rigid. This externally breaks the Galilean invariance and a large scale z-invariant horizontal velocity is not allowed by the boundary conditions. However, for low Prandtl number fluids, the oscillatory instability occurs only slightly above the

convection onset, and we thus hope to be able to model the dominant effect of rigid boundaries by extending phenomenologically eqs. (9): to wit, we incorporate a damping term $-\nu\psi$ in the right-hand side of eq. (9b); note that the large scale horizontal velocity field is now of the form $Q(z)\psi(Y, T)$, where $Q(z)$ satisfies the boundary conditions. In other words, the vertical vorticity modes are damped. We assume that the ensemble of these modes acts like one mode on the average. We can estimate the overall damping by the one of the least damped mode (the first Fourier mode in z with a vanishing horizontal wavenumber) which gives $\nu \approx P\pi^2$. We do not consider the nonlinear renormalization of this damping by a term of the form $\psi\phi_Y^2$ because we expect its coefficient to vanish since ν does not depend on α (see below). We thus obtain for the phase gradients θ and χ

$$\theta_T = \chi, \tag{16a}$$

$$\chi_T = -\nu\chi + \partial_{YY}\big[a\theta + b\chi - c\theta_{YY}$$
$$- d\chi_{YY} + g_1\theta^3 + g_2\theta^2\chi\big], \tag{16b}$$

where g_1 and g_2 obey the same equations as in the stress-free case (15a, b).

The growth-rate η of the oscillatory instability obeys the dispersion relation

$$\eta^2 + (\nu + bk^2 + dk^4)\eta + ak^2 + ck^4 = \mathcal{O}(k^4). \tag{17}$$

Stability at short wavelengths requires $d > 0$. The oscillatory instability occurs for

$$b_0 = -2(\nu d)^{1/2}, \tag{18a}$$

with a finite wavenumber

$$k_0 = (\nu/d)^{1/4} \tag{18b}$$

and a frequency at onset

$$\omega_0 = \big[a(\nu/d)^{1/2} + c(\nu/d)\big]^{1/2}. \tag{18c}$$

The real and imaginary parts of the growth-rate at the oscillatory instability onset, as a function of the disturbance wavenumber are given in figs. 2 and 3 of the next section. We observe that the oscillatory instability comes from the interaction between the neutral translation mode ($\eta(0) = 0$), and the damped Galilean mode ($\eta(0) = -\nu$). The oscillatory instability occurs at a finite wavenumber k_0 because of the external damping due to rigid boundary conditions.

3.2. Nonlinear evolution of the oscillatory instability

The main questions about the nonlinear evolution of the oscillatory instability are:
– Is the bifurcation supercritical or subcritical?
– Why are standing waves not observed, experimentally or in direct numerical simulations, at the oscillatory instability onset?

In the vicinity of the instability onset, the envelope equation technique can be used to describe the post bifurcation stage; thus we write

$$\theta(Y, T) = A(\zeta, \tau)\exp i(\omega_0 T + k_0 Y)$$
$$+ B(\zeta, \tau)\exp i(\omega_0 T - k_0 Y) + \text{c.c.}$$
$$+ C(\zeta, \tau) + \cdots. \tag{19}$$

The fields A and B describe the slowly varying amplitudes (in Y and T) of the waves that propagate to the right and to the left. The field C takes into account the existence of marginal modes for $k \to 0$. Using standard asymptotic methods [25], we obtain at leading order the evolution equations for A, B, C:

$$A_\tau = (k_0^2/2)(b_0 - b)A - \omega_1 A_\zeta + (\xi_0^2 - i\omega_2)A_{\zeta\zeta}$$
$$- (\beta - i\gamma)\big[3|A|^2 + 6|B|^2 + 3C^2\big]A + \cdots, \tag{20a}$$

$$B_\tau = (k_0^2/2)(b_0 - b)B + \omega_1 B_\zeta + (\xi_0^2 - i\omega_2)B_{\zeta\zeta}$$
$$- (\beta - i\gamma)\big[6|A|^2 + 3|B|^2 + 3C^2\big]B + \cdots, \tag{20b}$$

$$C_\tau = (a/\nu)C_{\zeta\zeta} + \cdots, \tag{20c}$$

with

$$\omega_1 = (k_0/\omega_0)(a + 2ck_0^2),$$

$$\omega_2 = (1/2\omega_0)\Big[(a + 6ck_0^2)$$
$$- (k_0/\omega_0)^2(a + 2ck_0^2)^2\Big],$$

$$\xi_0^2 = 2(\nu d)^{1/2},$$

$$\beta = -(k_0^2 g_2)/2,$$

$$\gamma = (k_0^2 g_1)/2\omega_0.$$

C is coupled with A and B only through higher order nonlinear terms $(C|A|^2_{\xi\xi}, C|B|^2_{\xi\xi}, \ldots)$, and thus is damped in the vicinity of the oscillatory instability onset. The bifurcation is supercritical if

$$g_2 = (\alpha/2)\,\partial b/\partial\alpha > 0.$$

The sign of g_2 depends on the wavenumber of the basic pattern and on the fluid Prandtl number (see section 4). Thus the oscillatory instability is a supercritical or subcritical bifurcation depending on α and P.

In the supercritical case, eqs. (19) have spatially homogeneous solutions

$$A_0(\tau) = P \exp i\Omega\tau,$$

$$B_0(\tau) = Q \exp i\Omega\tau,$$

that describe either propagating waves:

$$P^2 = k_0^2(b_0 - b)/6\alpha, \quad Q^2 = 0,$$

$$\Omega = k_0^2(b_0 - b)\beta/2\alpha;$$

$$P^2 = 0, \quad Q^2 = k_0^2(b_0 - b)/6\alpha,$$

$$\Omega = k_0^2(b_0 - b)\beta/2\alpha.$$

or standing waves:

$$P^2 = Q^2 = k_0^2(b_0 - b)/18\alpha,$$

$$\Omega = k_0^2(b_0 - b)\beta/2\alpha.$$

Only the former are stable because the coefficients of the self-interaction nonlinear terms, $|A|^2A$ and

$|B|^2B$, are smaller than those of the cross terms, $|A|^2B$ and $|B|^2A$. Therefore propagating waves are selected at the oscillatory instability onset, in agreement with experimental observations [17] and direct numerical simulations [18–20, 27]. Note that this result depends only on the form of the phase equations (16), and not on the numerical values of the coefficients.

4. Numerical evaluation of the phase equation coefficients for rigid boundary conditions

In this section we compute the numerical values of the coefficients that control both linear and nonlinear phase dynamics in the case of convection with rigid boundary conditions (see eqs. (16)). This quantitative study provides information regarding whether the oscillatory instability is a supercritical or subcritical bifurcation, as well as various scaling laws for the Prandtl number dependence of the frequency and wavenumber at onset. We have used the code of Clever and Busse for steady nonlinear thermal convection with rigid boundary conditions, as well as their code for the linear stability analysis of the nonlinear steady state. For a summary of their derivation and formalism we refer the reader to their paper [2]. To insure accuracy of the steady solution and the stability analysis, a truncation of $N = 10$ (which involves 75 modes) has been used for all the calculations reported here. This truncation enables one to determine R_0, the Rayleigh number for the onset of the oscillatory instability, to within 0.1% for the ranges of R, P and α considered (as long as parabolic interpolation is used with $\Delta k \le 0.2$, $\Delta R \le 100$, $\Delta\alpha \le 0.15$).

R_0 was calculated as follows: at each of several Rayleigh numbers near R_0, the growth-rate $\eta(k)$ was computed from the linear stability code for several values of k near k_0. A parabola was fit to $\text{Re}[\eta(k)]$ to find $\text{Re}[\eta]_{\text{max}}$ for each R. Fitting a parabola to $\text{Re}[\eta]_{\text{max}}(R)$ then yields R_0 as a root. In this procedure, α and P were fixed.
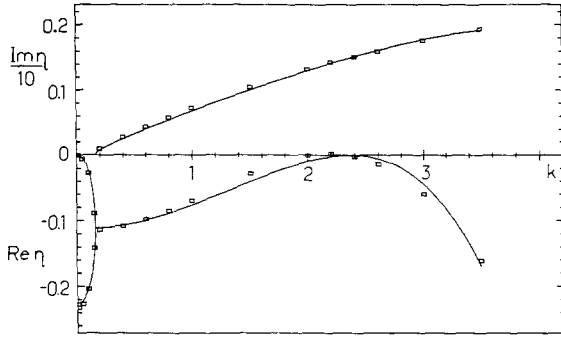
Fig. 2. A plot of the complex growth-rates (lower-half of the figure: real part of the growth-rate, upper-half: imaginary part divided by 10) versus the disturbance wavenumber k. The boxes are the growth-rates for the oscillatory instability, obtained numerically from the Oberbeck–Boussinesq equations ($R = 1888$, $P = 0.025$, $\alpha = 3.117$). The solid lines correspond to polynomial fits, up to fourth order in k, to the sum and product of the roots of eq. (17), yielding the values, $\nu = 0.226$, $a = 0.482$, $b = -0.0816$, $c = -0.0146$, $d = 7.42 \times 10^{-3}$. The mean quadratic error is 1.62×10^{-4} for the sum, and 1.64×10^{-3} for the product.
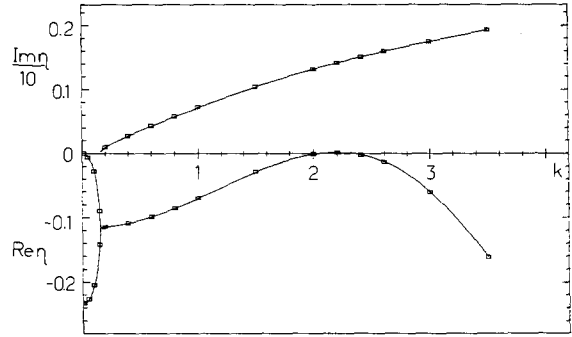
Fig. 3. Same as fig. 2, except that the fit is now up to 6th order, which yields: $\nu = 0.233$, $a = 0.550$, $b = -0.107$, $c = -0.0330$, $d = 0.0138$, $e = -3.64 \times 10^{-4}$, $f = 1.07 \times 10^{-3}$. The mean quadratic error is 2.81×10^{-7} for the sum, and 1.91×10^{-5} for the product.

4.1. Calculation of phase equations coefficients from $\eta(k)$

In order to extract from the computed values of $\mathrm{Re}(\eta)$ and $\mathrm{Im}(\eta)$ information on such quantities as ν, a, b, c, d (see eq. (16)) we have analyzed the data in terms of an assumed functional form for $\mathrm{Re}(\eta)$ and $\mathrm{Im}(\eta)$. More precisely, as a consequence of our model (see eq. (17)) one has

$$\nu + bk^2 + dk^4 = -S(k), \tag{21a}$$

$$ak^2 + ck^4 = P(k), \tag{21b}$$

where $S(k)$ and $P(k)$ stand for the sum and the product of the complex growth-rates. It is tempting to use this relation to determine ν, a, b, c, d by polynomial least squares fits to S and P. The result of such a fit is shown in fig. 2. Let us remark that our model captures both the small-k bifurcation of the growth-rates and their high-k behavior, with a minimum number of parameters. A direct polynomial fit of the growth-rates themselves can-

not cope with the small-k bifurcation. This gives strong support to the linear part of our model. Note that, although the fit appears to be rather good, systematic errors are nevertheless present, suggesting that higher orders in k have to be retained.

The result of a 6th order fit, using

$$\nu + bk^2 + dk^4 + ek^6 = -S(k), \tag{22a}$$

$$ak^2 + ck^4 + fk^6 = P(k), \tag{22b}$$

instead of (21) is shown in fig. 3. Note that the quantitative agreement is much better with 6th order fit than with 4th order as witnessed for instance by a two order of magnitude decrease for the mean quadratic errors (see captions of figs. 2 and 3).

The "linear" coefficients (ν, a, b, c, d) and the "nonlinear" coefficients (g_1, g_2) of eq. (16) are functions of the parameters R, P and α. Even though a full exploration of the three-dimensional parameter space is prohibitively expensive, the general dependence of the coefficients can be understood by their behavior when two parameters are fixed and the third is allowed to vary. We also have examined the linear coefficient dependence along $R_0(P)$ for fixed α. The study of the R and

P dependences of the nonlinear coefficients was even more limited, as eq. (15) implies the need of $\eta(k)$ profiles for several α values. We commence the discussion of the numerical results by looking at the Prandtl number dependence followed by dependence upon R and α.

4.2. Prandtl number dependence at $R = 1800$

Although we shall see that the P-dependence of the coefficients is more remarkable when evaluated at R_0, we describe here the dependence at $R = 1800$, $\alpha = 3.117$ (the critical wavenumber for convective onset). In the range of Prandtl numbers examined (0.01 to 0.2), the coefficient v is the only one to clearly follow a power-law form ($v \sim P$). The other linear coefficients have extrema. Although the 4th and 6th order fits yield different values, we can say that a_{max} occurs for $P > 0.2$, $|b|_{max}$ is near $P = 0.05$, $|c|_{max}$ is near $P = 0.1$ and d_{max} is around $0.1 \leq P \leq 0.2$. For Prandtl numbers above those of these "maxima", the coefficients eventually change sign. These sign changes all occur when $R = 1800$ is well below that of the onset value of R_0. From the tendencies exhibited as P decreases toward $P = 0.01$ from above, we speculate that the low Prandtl number limit would show b, $d \sim P$ and a, $c \sim P^2$.

4.3. Prandtl number dependence at R_0

The Rayleigh number for the onset of the oscillatory instability, R_0, is itself a complicated function of P and α. However, if one evaluates the linear coefficients at $R_0(P)$ for fixed α, one finds a remarkable power-law dependence [28] (see fig. 4, for which $\alpha = 3.117$).

$$v = \sigma_v P, \quad a = \sigma_a P^2, \quad b = \sigma_b P, \quad c = \sigma_c P^2,$$

$$d = \sigma_d P, \quad e = \sigma_e P, \quad f = \sigma_f P^2.$$

Evaluating the coefficients to two significant figures, at $P = 0.025$ and $R = 1886.4$ yields
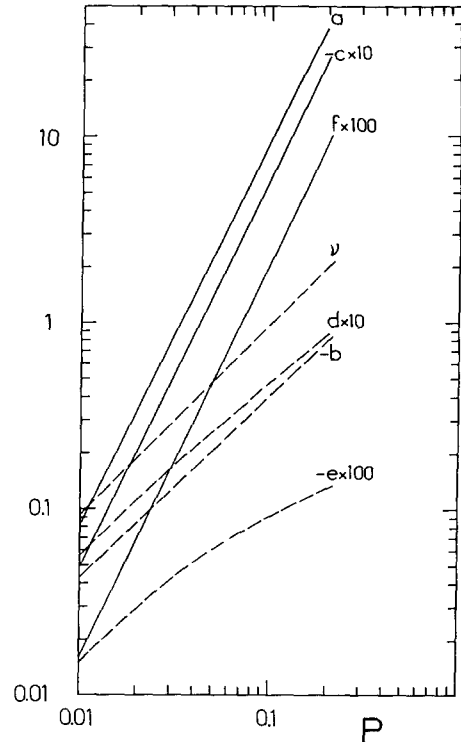

Fig. 4. Prandtl number dependence of the coefficients of the linearized phase equation along $R_0(P)$ for $\alpha = 3.117$ (6th order fit).

	4th order fit	6th order fit
$\sigma_v =$	9.0	9.3
$\sigma_a =$	760	870
$\sigma_b =$	-3.2	-4.2
$\sigma_c =$	-26	-52
$\sigma_d =$	0.29	0.55
$\sigma_e =$	—	-0.015
$\sigma_f =$	—	1.7

Several important relations may be deduced from the power-law behavior. From eqs. (18) we can expect (for fixed α) that the critical wavenumber k_0 at the oscillatory instability onset (i.e. the disturbance wavenumber where the hump in Re η just becomes zero) is independent of P. In addition, the oscillatory frequency at onset is directly proportional to P.

	4th order	6th order	Stability code
$k_0 =$	2.35	2.18	2.16
$\omega_0 =$	$58P$	$55.9P$	$55.6P$

We also note that k_b, the value of the disturbance wavenumber for the merging of the two real eigenvalues to form the complex conjugate pair, is obtained form $\Delta = (\nu + bk^2 + dk^4)^2 - 4(ak^2 + ck^4) = 0$. Factoring out P^2 from the power law dependencies reveals that k_b is also independent of P along $R_0(P)$.

Some comments on accuracy are in order. It is clear from figs. 2 and 3 that the model nicely fits the instability growth-rate curves $\eta(k)$. The 6th order fit is of course much better quantitatively. Although there are rather large discrepancies between the coefficients from the two fitting orders, the signs and power law relations are well preserved in each case. Given the method by which R_0 was calculated directly from $\eta(k)$ near k_0, it is more accurate than what one could find using the relation $b = -2\sqrt{(\nu d)}$. Although different grid choices for k can influence the coefficient values obtained, for a given fit order, these coefficients are reproducible to within 10% for any reasonable k-grid choice.

4.4. Rayleigh number dependence

We have investigated the Rayleigh number dependence of the linear coefficients for $P = 0.01$, 0.025, 0.05, 0.1 and 0.2 and $\alpha = 3.117$. The coefficient ν is essentially independent of R, except for a very slight decrease of ν with increasing R for $P = 0.01$.

Supposing that $a \sim [(R - Rc)/Rc]^{n_a}$, and similarly for b, c and d, we find that $1 \leq n_a$, $n_c \leq 2$, and $0.3 \leq n_b$, $n_d \leq 1.0$ with $n_d < n_b$. Each of these n's generally decreases with increasing P.

4.5. Dependence upon the basic state wavenumber α

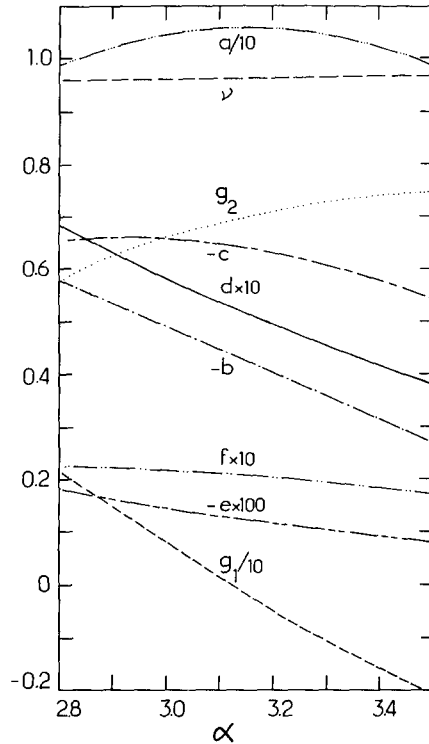The dependence of various coefficients upon the basic state roll wavenumber α is shown for $P = 0.1$

Fig. 5. Dependence of the phase equation coefficients with respect to the roll pattern wavenumber α, for $P = 0.1$ and $R = 2400$ (6th order fit).

and $P = 0.025$ in figs. 5 and 6, respectively. The coefficient ν is relatively insensitive to change in α. Of special significance is the minimum in $b(\alpha)$ for $P = 0.025$, which implies that g_2 will change sign near $\alpha = 2.94$ (6th order fit). We present the stability diagram for mercury ($P = 0.025$) in fig. 7. Above the curve, oscillating convection should occur. To the right of the nearly vertical dashed line ($\alpha \approx 2.94$, 6th order fit), we have $g_2 > 0$ (supercritical onset) while on the left $g_2 < 0$ (subcritical onset). The dotted line represents the result of the fourth order fit. For $P = 0.025$, the critical wavenumber for onset of the instability along the linear onset curve follows the form, $k_0 = 0.0986\alpha + 1.86$, and the frequency $\omega_0 = 0.242\alpha^2 - 0.362\alpha + 0.166$, (between $\alpha = 2.8$ and $\alpha = 3.1$). For the critical wavenumber for convection onset ($\alpha_c = 3.117$), the transition to oscillatory convection is
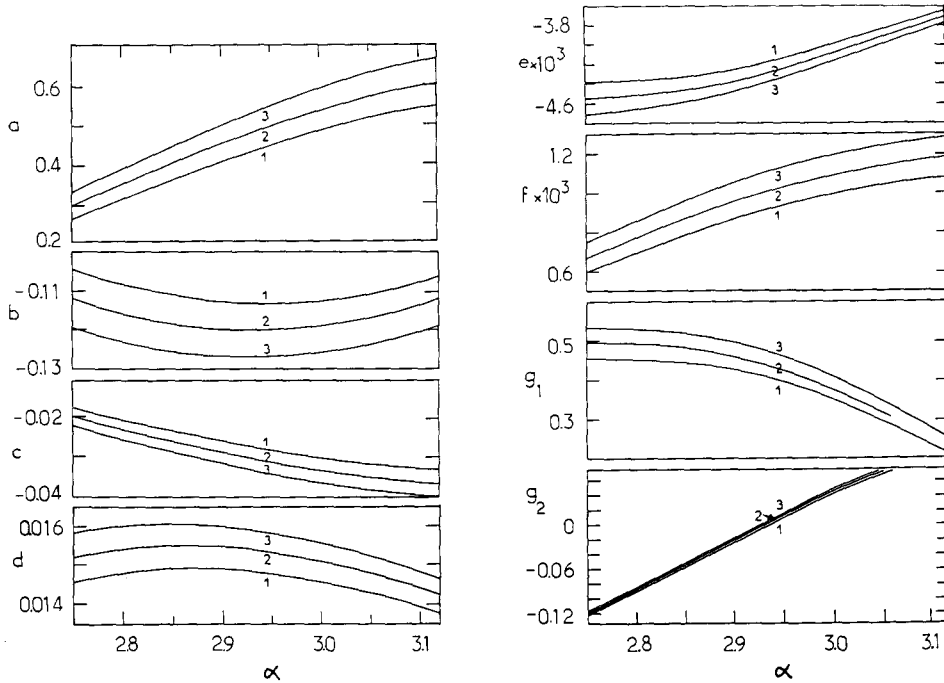
Fig. 6. Same as fig. 5 for $P = 0.025$; the curves labelled (1), (2) and (3) correspond to different values of the Rayleigh number $R = 1888$, 1898 and 1908 (6th order fit).
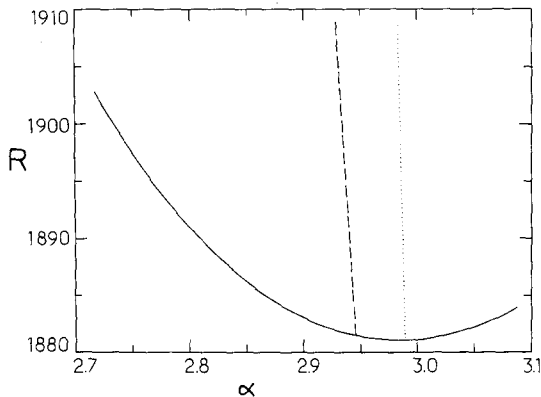

Fig. 7. Onset curve $R_0(\alpha)$ for the oscillatory instability for $P = 0.025$; above $R_0(\alpha)$ the oscillatory instability is linearly unstable; the onset is subcritical to the left of the dashed curve (6th order fit), respectively to the left of the dotted curve (4th order fit), whereas it is supercritical to the right.

supercritical; the oscillation amplitude increases like $(R - R_0)^{1/2}$, in agreement with experimental observations [26]. When the basic pattern wavenumber is constrained at $\alpha < \alpha_T$, we find that our model predicts subcritical onset for the oscillatory

instability in mercury ($\alpha_T = 2.99$ for the 4th order fit and $\alpha_T = 2.94$ for the 6th order fit). Higher order terms may change the precise value of α_T. In the case of subcritical onset our model does not describe the nonlinear oscillatory regime, and we cannot compare the evolution of its frequency with calculations of Clever and Busse ($P = 0.025$, $\alpha = 2.9$) [27], as higher order coefficients are needed for damping in the case of subcritical onset.

5. Conclusion

We have shown in this paper that the method of phase dynamics is a powerful tool to describe the nonlinear evolution of a secondary instability in a cellular flow. However, this formalism requires that the modeled instability has a zero growth rate for vanishing disturbance wavenumber. This is usually the case when the secondary instability traces back to a continuous broken symmetry at

the primary instability onset, but we cannot make predictions for the oscillatory "thermal blob" type instabilities [5], since these instabilities typically have finite growth rates at zero disturbance wavenumber. Moreover they have intricate vertical structure, which is beyond the reach of the vertically averaged phase equation approach.

The effect of the fluid container lateral boundaries also appears as a severe limitation of the validity of phase dynamics, since they externally break both translational and Galilean invariances. However, the predictions of numerical stability analysis in infinite geometry [2–5] are in good agreement with experimental observations [17, 29] when the fluid container aspect ratio is large enough; the onset value for the oscillatory instability in mercury, with a parallelepipedic container of dimensions 5.00 cm by 3.50 cm by 0.48 cm high, is less than 20% larger than the theoretical value [26]. We thus expect the phase dynamics approach to be correct in the large aspect ratio limit.

Finally, some comments on the low Prandtl number limit are in order; as $P \rightarrow 0$, the oscillatory instability critical wavenumber remains finite, and thus, we cannot ensure asymptotically the validity of our model for rigid boundary conditions. However, its qualitative predictions, supercritical oscillatory instability onset and finite amplitude travelling waves (for a roll wavenumber equal to the critical wavenumber for the onset of convection), are in agreement with experimental observations. Moreover, the model is in quantitative agreement with the numerical computation of the oscillatory instability growth-rate, and the effect of higher order terms (in the instability wavenumber) is small, which shows numerically that the phase dynamics approach is correct.

Acknowledgements

References

[1] A. Schlüter, D. Lortz and F. Busse, J. Fluid Mech. 23 (1965) 129–144.

[2] R.M. Clever and F.H. Busse, J. Fluid Mech. 65 (1974) 625–645.

[3] F.H. Busse and R.M. Clever, J. Fluid Mech. 91 (1979) 319–335.

[4] E.W. Bolton and F.H. Busse, J. Fluid Mech. 150 (1985) 487–498.

[5] E.W. Bolton, F.H. Busse and R.M. Clever, J. Fluid Mech. 164 (1986) 469–485.

[6] For a review, see Y. Kuramoto, Prog. Theor. Phys. 71 (1984) 1182–1196.

[7] P. Ortoleva and J. Ross, J. Chem. Phys. 58 (1973) 5673–5680.

[8] Y. Kuramoto and T. Tsuzuki, Prog. Theor. Phys. 55 (1976) 356–369.

[9] L.N. Howard and N. Kopell, Stud. Appl. Math. 56 (1977) 95–145.

[10] Y. Pomeau and P. Manneville, J. Physique Lettres 40 (1979) 609–612.

[11] M.C. Cross, Phys. Rev. A 27 (1983) 490–498.

[12] M.C. Cross and A.C. Newell, Physica 10D (1984) 299–328.

[13] F. Busse, J. Fluid Mech. 52 (1972) 97–112.

[14] E.D. Siggia and A. Zippelius, Phys. Rev. Lett. 47 (1981) 835–838.

[15] B.F. Edwards and A.L. Fetter, Phys. Fluids 27 (1984) 2795–2802.

[16] P. Coullet and S. Fauve, Phys. Rev. Lett. 55 (1985) 2857–2859.

[17] G.E. Willis and J.W. Deardorff, J. Fluid Mech. 44 (1970) 661–672.

[18] F.B. Lipps, J. Fluid Mech. 75 (1976) 113–148.

[19] J.B. McLaughlin and S.A. Orszag, J. Fluid Mech. 122 (1982) 123–142.

[20] M. Meneguzzi, C. Sulem, P.L. Sulem and O. Thual, submitted to J. Fluid Mech. (1985).

[21] A.C. Newell and J.A. Whitehead, J. Fluid Mech. 38 (1969) 279–303.

[22] L.A. Segel, J. Fluid Mech. 38 (1969) 203–224.

[23] V.I. Arnold, Supplementary Chapters to the Theory of Ordinary Differential Equations, (Nauka, Moscow, 1978).

[24] J. Guckenheimer and P. Holmes, Nonlinear Oscillations, Dynamical System and Bifurcation of Vector Fields (Springer, Berlin, 1984).

[25] A.C. Newell, Lectures in Appl. Math. 15 (1974) 157–163.

[26] S. Fauve, thesis, Paris (1984).

[27] R.M. Clever and F.H. Busse, J. Fluid Mech. 176 (1987) 403–417.

[28] Note that P can be factored out everywhere by choosing a viscous time-scale instead of a thermal time-scale.

[29] J.P. Gollub, A.R. McCarriar and J.F. Steinman, J. Fluid Mech. 125 (1982) 259–281.